

# Infrared Detector Systems at ESO

Gert Finger\*, Reinhold J. Dorn, Siegfried Eschbaumer, Derek Ives, Leander Mehrgan,  
Manfred Meyer and Jörg Stegmeier.  
European Southern Observatory, Karl-Schwarzschild-Strasse 2, D-85748-Garching, Germany.

## ABSTRACT

Complementary to the overview of the optical detector projects, this paper lists the infrared projects that have been started or completed at ESO since the DfA2005 workshop [1]. New detector developments for the mid-infrared, the implementation of innovative near infrared avalanche photo diode array designs for AO wavefront sensing and interferometry and novel detector controllers on a single chip will be discussed as well. Reference will be made to the topics which are presented in more detail in other contributions to DfA2009 [2].

**Keywords:** infrared arrays, infrared mosaic, mid infrared, near infrared, avalanche photo diode, ASIC, adaptive optics, fringe tracking, HgCdTe, readout noise, threshold limited integration, HAWAII-2RG, VIRGO

## 1. INTRODUCTION

Since the last detector workshop in Taormina (DfA2005), infrared focal plane technology has evolved further and large infrared arrays and mosaics are now in routine operation at the VLT telescopes and at the VISTA survey telescope on Paranal. The first of the second generation VLT instruments, X-Shooter, which is equipped with a 2Kx2K NIR HgCdTe array, is now complete and two new instruments, KMOS and SPHERE, are under construction and will be equipped with the same array types. The performance of the mid-infrared instrument, VISIR is inadequate because of the detector performance. Therefore, a new Si:As array is being developed. At present, high speed infrared applications such as tip-tilt, wavefront and fringe sensing in interferometers utilize PICNIC or Hawaii1 detectors which are limited by the intrinsic noise floor of the CMOS readout multiplexers. This noise barrier can only be overcome by employing additional processes such as the photon avalanche effect. To this end, ESO has initiated the development of an eAPD array. This paper will describe this development along with some promising early results.

## 2. HAWK-I

HAWK-I is the new High-Acuity Wide-field K-band Imager for ESO's Very Large Telescope [3]. It is equipped with a mosaic of four 2K × 2K arrays covering the wavelength range from 0.9–2.4 μm. The imager has a field of view of 7.5' × 7.5' with 0.1" pixels. The camera uses only reflective optics. The filters have excellent throughput and the detectors have quantum efficiencies exceeding 80% over the entire spectral range [4]. This results in an extremely high overall throughput of ~ 60% in Y, J and H band and ~50% in K-band which includes the QE of detectors.

The four detectors of the HAWK-I mosaic are 2K × 2K Rockwell Hawaii-2RG HgCdTe MBE arrays with 2.5 μm cutoff. The arrays are grown on a CdZnTe substrate which has not been removed. The mosaic mount is the standard GL scientific mosaic package developed for the JWST. It is shown in the left image of Figure 1. The four fan-out boards with filters and antistatic protection for clocks and bias voltages and the preamplifiers for the 132 video channels of the mosaic (4 x 32 video channels + 4x1 channels for the guide window) are contained in the two aluminum boxes

\*gfinger@eso.org; phone +49-89-32006256; fax +49-89-3202362; [www.eso.org/~gfinger](http://www.eso.org/~gfinger)

on the back side of the mosaic close to the detectors as shown in the right image of Figure 1. The design of the cold preamplifiers is symmetric to form a true differential signal chain [6]. The preamplifiers are built with linear CMOS opamps (LinCMOS TLC2274) which work well at detector temperatures as low as 40 K.

The IRACE acquisition system can read all 132 channels simultaneously. This allows the readout of the full detector mosaic in 1.3 seconds which is adequate for all HAWK-I applications. For the foreseen ground-layer adaptive optics system which is expected with the advent of the VLT adaptive secondary mirror in 2012, a fast read out of a guide window is available to acquire a Natural Guide Star and perform the tip-tilt correction at frequencies of about 100 Hz.

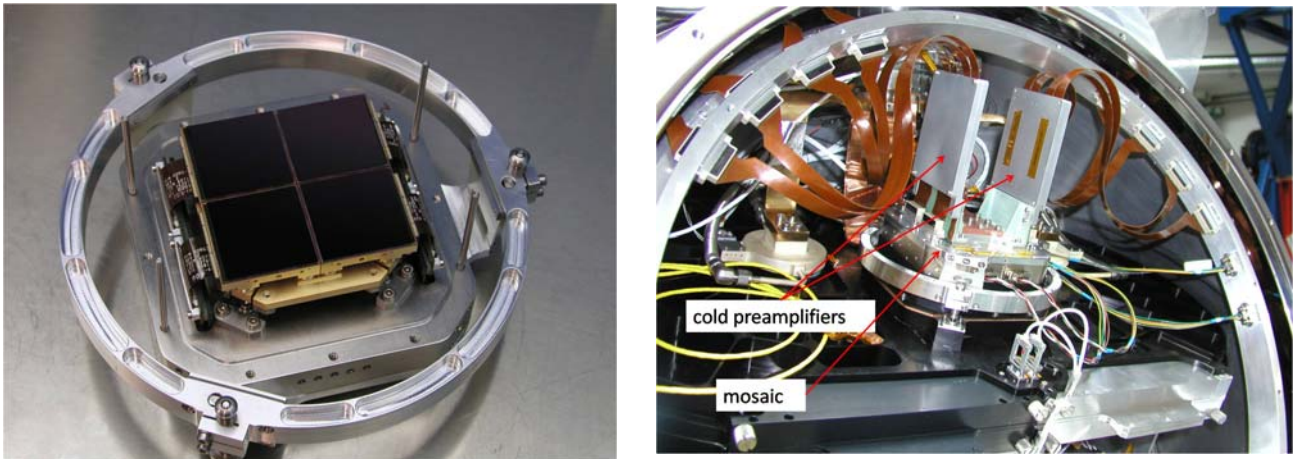


**Figure 1** HAWK-I mosaic with 2x2 2Kx2K Hawaii-2RG  $\lambda_c=2.5 \mu\text{m}$  MBE arrays. Left: front side of GL scientific mosaic package mounted in alignment ring for focus and tip-tilt adjustment. Right: backside of mosaic mount with cold CMOS preamplifier boards for 132 video channels and flex boards as mounted in the HAWK-I instrument.

In HAWK-I, novel readout modes were tested on sky such as tip tilt correction with the guide window or threshold limited integration (TLI) which allows to extend the dynamic range of the detector. The TLI mode can easily be implemented in the sample-up-the-ramp or nondestructive readout mode which is the default mode of all IR detectors in ESO instruments [4].

### 3. VISTA

The VISTA Infrared Camera is a large survey camera built for a dedicated 4 meter telescope on Paranal (Visible and Infrared Survey Telescope for Astronomy VISTA). The camera has a field of view of 1.65 degrees with a pixel scale of 0.34". It has a large filter wheel with broad band filters for Z,Y,J,H and Ks band imaging [7]. The distinctive feature of VISTA is the fact that it has no reimaging optics and provides only image correction for the f/3.25 beam of the telescope. The camera has no cold pupil stop. Instead, it uses a set of cold baffles to block out the warm telescope and background radiation as shown in the left image of Figure 2. The baffles have a solar coating which absorbs wavelengths shortward of  $3\mu\text{m}$  and is highly reflective longward of  $3\mu\text{m}$ . This coating serves two purposes. It reduces stray light and reduces the cooling of the entrance window.

The focal plane of VISTA has 64 Megapixels and is the largest infrared focal plane in operation at any telescope. It consists of 16 Raytheon VIRGO 2Kx2K HgCdTe LPE arrays with  $2.5 \mu\text{m}$  cutoff grown on a CdZnTe substrate. The arrays are mounted in the focal plane in a sparse mosaic configuration with the gaps between detectors being smaller than the size of the individual array (see right image in Figure 2). The mean quantum efficiencies of the 16 detectors have been measured as (J,H,K)=(90,96,92)%, the mean dark current is 1.2 e/pixel/s and the mean readout noise is 20.9 e-rms. The well-depths for the arrays range between 110,000 and 180,000 electrons [8].

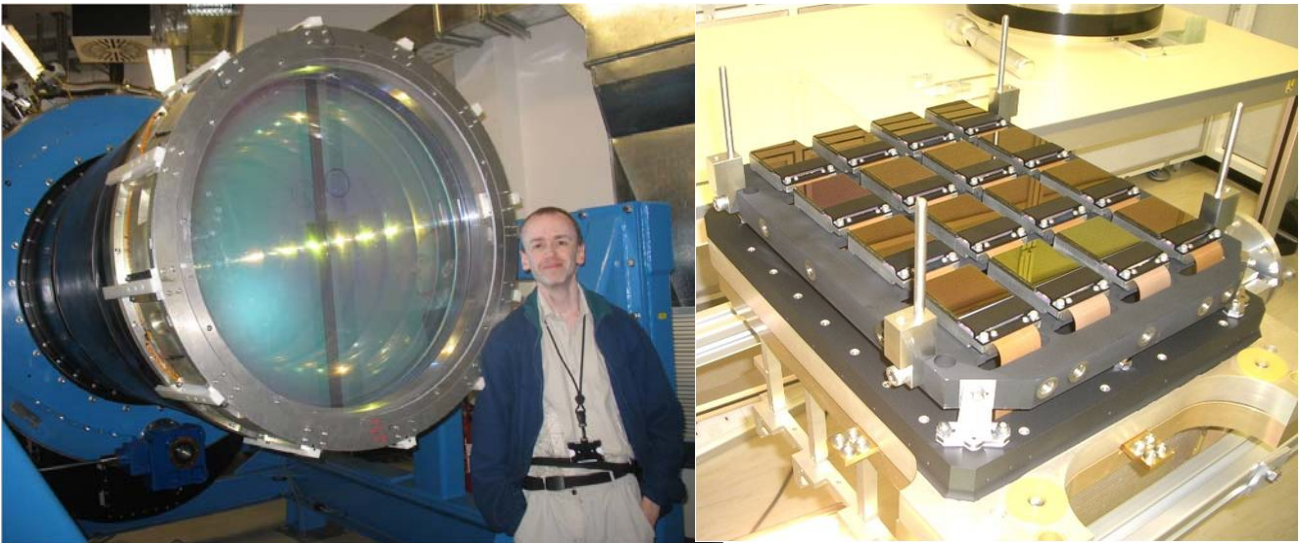


**Figure 2: VISTA camera. Left: entrance window with baffle system. Right: VISTA mosaic of 4x4 2Kx2K Raytheon VIRGO LPE HgCdTe arrays.**

All detectors are read out simultaneously by the standard ESO infrared control electronics IRACE with a total of 256 simultaneous readout channels [9]. The complete focal plane can be read in less than 1 second. The cold preamplifiers use a design similar to the one used for HAWKI as described above. The 256 channel cryo amplifiers are located on four PCBs on the back of the FPA frame. In operation they reliably deliver robust low noise performance. Just on time for the DfA2009 detector workshop spectacular first light images taken with the VISTA camera were published [10]. One example is shown in Figure 3.

#### 4. X-SHOOTER

X-shooter is the first of the second generation VLT instruments [11]. It is a high-efficiency spectrograph observing the complete spectral range between 300 nm and 2500 nm in a single exposure with a spectral resolving power  $R > 5000$ . The instrument is located at the Cassegrain focus of one of the VLT telescopes and consists of three cross-dispersed spectrographs: UV, VIS and Near-IR. Each spectrograph has a fixed echelle grating and prism cross-dispersers. The light is distributed to the 3 spectrographs by 2 dichroics. The near infrared arm covers the wavelength range from 1 – 2.5  $\mu\text{m}$  and is cooled by a liquid nitrogen bath cryostat [12]. The focal plane is equipped with a single Hawaii-2RG detector. Only 1Kx2K pixels are needed for the optical field. The detector operates at 81 K.

During instrument assembly, integration and test (AIT) a science grade array was used which still had a CdZnTe substrate. This substrate acts like a Fabry-Perot generating serious fringing with a fringe contrast of 1.4 as shown in the upper image of Figure 4. The fringe separation and the refractive index of CdZnTe yielded the correct calculated value for the substrate thickness of 862  $\mu\text{m}$ . Since the spectrograph has flexure, fringing seriously reduces the advantage of flatfielding. Fortunately, at the time of AIT a substrate-removed engineering array was already available. Replacing the science array with the substrate-removed engineering array effectively eliminated fringing as can be seen in the lower image of Figure 4. Since the engineering array had a science grade 2Kx1K area it was decided to permanently install this array in the instrument [4].

Threshold-limited integration (see chapter 2) was implemented in X-shooter as well and proved to be particularly useful to cope with the high contrast of spectra taken with long deep exposures. Furthermore, a new mode called global reset

detrapping, which is a new mitigation strategy to reduce image persistence, was developed in X-Shooter and successfully tested on sky [5].



**Figure 3: First light image of VISTA taken through J, H and Ks filters. Star-forming region NGC 2024 in the constellation of Orion. The image shows about half the area of the full VISTA field and is about 40 x 50 arcminutes in extent. Total exposure time was 14 minutes. For details and high resolution image see: <http://www.eso.org/public/images/eso0949>.**

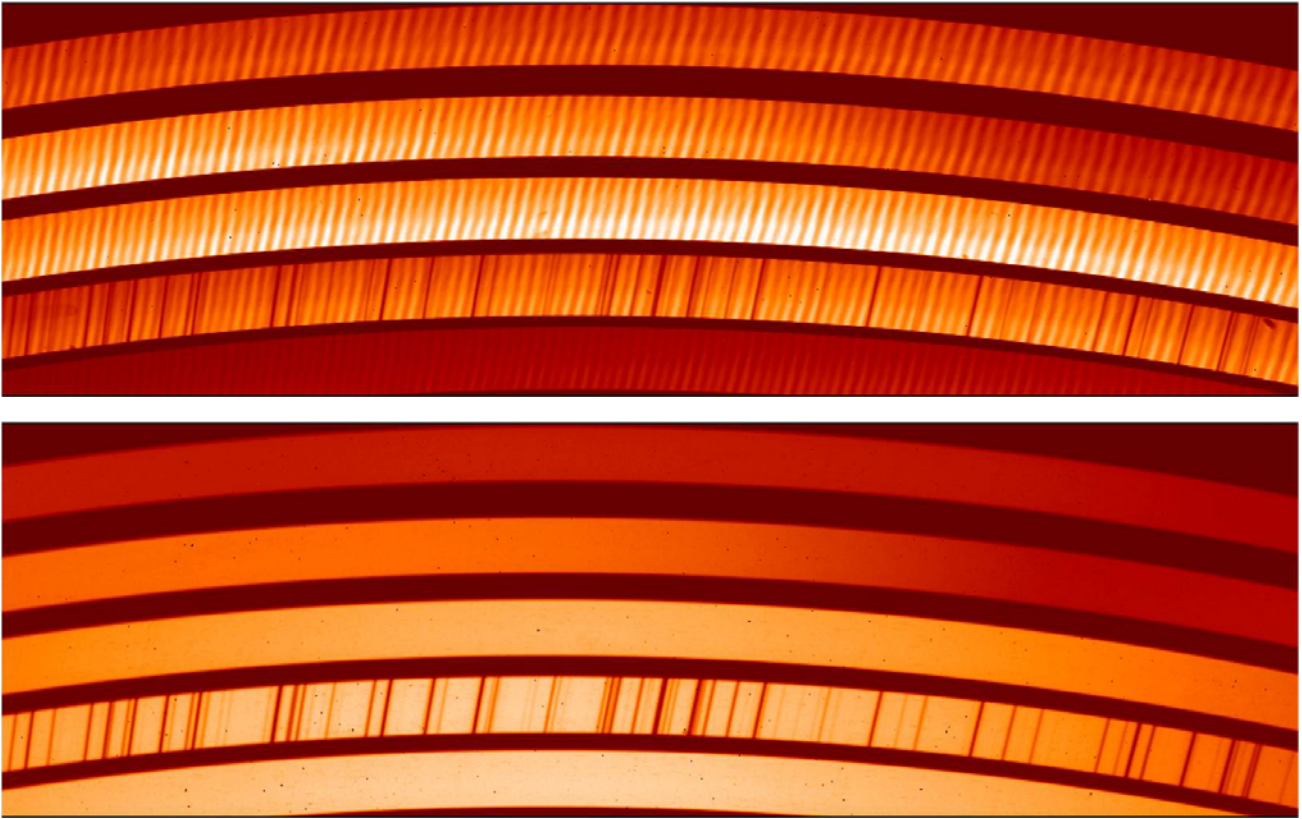


**Figure 4: Fringing in XSHOOTER. Top: Spectrum on Hawaii-2RG array and CdZnTe substrate, fringe contrast 1.4. Bottom: Spectrum with Hawaii-2RG array and CdZnTe substrate-removed, no fringing.**

## 5. KMOS

KMOS is a fully cryogenic near-infrared multi-object integral-field spectrometer which is another second-generation instrument currently under construction for the VLT [13][14]. The selection of objects is provided by 24 configurable pick-off arms that operate at cryogenic temperatures and position fold mirrors at user-specified locations in the Nasmyth focal plane (see left image in Figure 5). The sub-fields thus selected are then magnified onto 24 image slicer integral field units (IFU's) that partition each subfield into 14 identical slices, with 14 spatial pixels along each slice. Light from the IFUs is dispersed by three identical cryogenic grating spectrometers which generate 14 x 14 spectra, each with 1000 spectral resolution elements, for all of the 24 independent sub-fields. The focal plane of each spectrometer is equipped with a single 2Kx2K Hawaii-2RG substrate-removed HgCdTe detector. The detectors are mounted on a motorized focus stage (see right image in Figure 5). The three detectors of the spectrometers are clocked and read out simultaneously by the new 96-channel NGC system [15]. The readout time of all three detectors is less than a second.

The instrument is now in the AIT phase. First spectra have been obtained with the stand-alone spectrometer. The pick-off arms comply with all specifications, when operated at cryogenic temperatures. At the present time one spectrometer with the IFU and pick-off arms is being assembled for first end-to-end tests of the instrument.

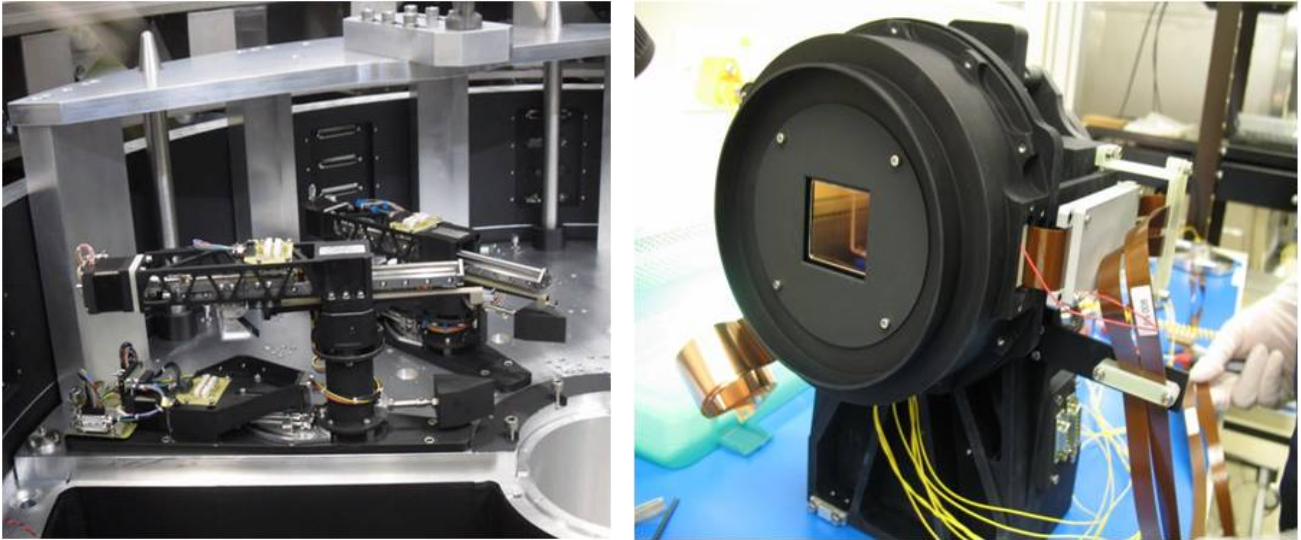


**Figure 5: Left: Cryogenic KMOS pick-off arms. Right: Hawaii-2RG array mounted on KMOS motorized focus stage with flex boards and preamplifiers in aluminum box on right side.**

## 6. SPHERE

The high contrast planet finder SPHERE is the third of the second-generation VLT instruments, which currently is undergoing AIT. SPHERE is built for direct detection of extra-solar planets [16]. The high spatial resolution will be delivered by SAXO, an extreme AO system with a deformable mirror having 41x41 actuators and a high contrast coronagraphic mask. The infrared detectors of SPHERE will be delivered with NGC data acquisition systems. The Differential Tip-Tilt loop which centers the beam on the coronagraphic mask and corrects for differential tip-tilt between the visible and the infrared channel requires an infrared sensor. The Hawaii1 1Kx1K Teledyne array was selected for this application. The NGC system directly interfaces to the SPARTA real time computer of the AO system. The differential imaging camera IRDIS operates in dual band imaging mode and provides images in two neighboring spectral channels. IRDIS is equipped with a single 2.5 micron cut-off Hawaii-2RG array of which only 1Kx2K pixels are used. The second instrument of SPHERE is the integral field spectrograph IFS. Even though the IFS only covers the spectral range of 0.95 to 1.65  $\mu\text{m}$ , a 2.5 micron cut-off Hawaii-2RG array was also selected for this instrument. This was done to minimize the manufacturing risk (2.5 micron material is a standard product) and to allow a larger number of detectors available for selection of the the best detector.

## 7. MID-INFRARED ARRAY DEVELOPMENT

The VLT mid-infrared instrument VISIR is currently equipped with two 256x256 Si:As blocked impurity band focal plane arrays from DRS Sensors. These arrays only exploit 25% of the VISIR focal plane which was oversized to allow upgrades to exploit future advances in detector technology. Since the current DRS detectors also exhibit several serious performance problems and limitations, due mainly to increased electronic noise and artifacts appearing at the low operating temperatures. For these reasons, ESO has launched a new development of a high flux 1Kx1K Si:As array for ground base applications at Raytheon Vision Systems. This array is called AQUARIUS and it is a derivative of the MIRI arrays developed for the James Webb Space Telescope [17]. The AQUARIUS detector will also be used in the VLTI interferometer instrument MATISSE. The unit cell design of the AQUARIUS array is a simple source follower per detector (SFD). The integrating node capacitance and thus the corresponding storage well and gain are switchable. The array has 64 video outputs, 32 at the bottom and 32 at the top, to give a possible frame rate of 120 Hz. The readout of a

window containing the central rows of the array is possible, but only complete rows can be read. The specifications for the AQUARIUS array are given in Table 1. First light with hybridized sensor chip assemblies have recently been achieved. A first light image is shown in Figure 6.

**Table 1:** Specifications of the Aquarius array

Parameter	Value
Format	1024 x 1024
Pixel Size	30 $\mu\text{m}$
Spectral range	5-28 $\mu\text{m}$
Readout Structure	SFD
Readout modes	Uncorrelated, double correlated, nondestructive
Mean Input Referred Noise (high gain, off-FPA CDS)	<1000 e-rms low gain < 100 e-rms high gain
Maximum Frame Rate	120 Hz
Number of Outputs	16, 64 (32 per side)
Windowing	Centered windowing
RQE at -2V bias $\lambda=3-5 \mu\text{m}$ $\lambda=8-14 \mu\text{m}$ $\lambda=16-22 \mu\text{m}$	>20% >50% w/AR coat >50% w/AR coat
Dark current	< 2 $10^3$ e/s/pixel
Typical Integration Capacity	
High Gain Low Gain	1 x $10^6$ e- 15 x $10^6$ e-
Operating Temperature	6 – 10 Kelvin
Power dissipation	100 mW
Packaging	124 pin LCC package

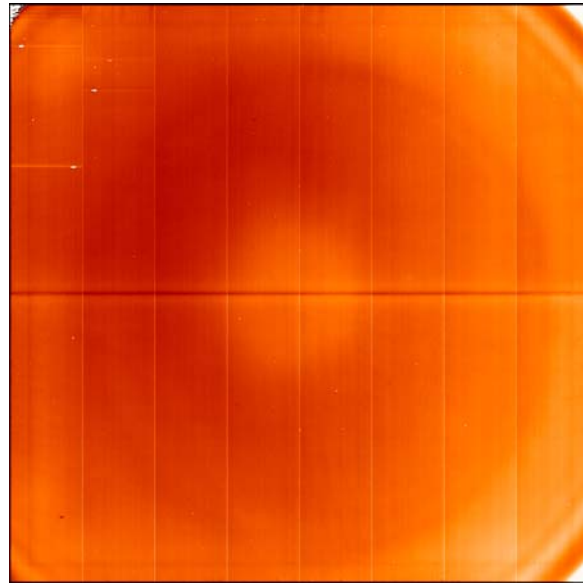


**Figure 6:** First light image with an AQUARIUS array obtained in 16 channel mode. Difference image of light source on and off.

## 8. ASIC DEVELOPMENT

At an early stage, ESO has procured a SIDECAR ASIC which has all the functionality of the FPA drive electronics as well as analog to digital conversion integrated on a single CMOS device [18]. The ASIC operates at cryogenic temperatures and can be placed next to the cold detector. It has a fully digital interface.

In a first step a 2K×2K silicon PIN diode array hybridized to a Hawaii-2RG multiplexer (HyViSI) was read out in 32-channel mode with the ASIC via the JADE2 card interface provided by Teledyne. The performance achieved with the ASIC and the standard ESO controller IRACE was comparable [19]. In a second step an FPGA based interface was developed at ESO which replaces the JADE2 card and seamlessly embeds the ASIC into the standard ESO environment of NGC which interfaces to a pci bus card and performs all real-time preprocessing on a Linux based PC. Thus the pci-bus interface and all the preprocessing tasks developed for NGC could be reused for the ASIC without modifications. At present, the interface uses only a single LVDS channel which minimizes throughput but an extension of the card functionality to 16 parallel data lines is planned, thus increasing the bandwidth to ~800Mbit. This will allow testing the fast output amplifiers of the H2RG detectors at 10 MHz pixel read speeds [20].

## 9. APD SENSORS FOR ADAPTIVE OPTICS

Infrared wavefront sensors of adaptive optics systems and fringe trackers in interferometers have to be read at frame rates of >1kHz to comply to the bandwidth requirements of the control loop. If no bright stars are in the field to be observed, signal levels are small and the performance of the control loop will be limited by the readout noise of the IR sensor. The sensors are hybridized to CMOS multiplexers which have an intrinsic noise level limiting the sensitivity of the system. In the past two decades since the introduction of the NICMOS array on Hubble there has been little progress in reducing the CMOS noise. Any noise improvement has been made through the reduction of the node capacitance by smaller pixels [22]. The readout noise is ~ 30 e-rms for PICNIC arrays operated at 220kHz/channel[21]. Several attempts have been made to improve this noise figure by designing more elaborate circuits in the pixel unit cells of the multiplexer using two-stage capacitive transimpedance amplifiers (CTIA). However, because of parasitic stray capacitance which is difficult to control, it is not easy to raise the conversion gain of the CTIA to a level of 1mV/electron and keep the detector output stable at high speed [23].

A new and promising approach to overcome the CMOS noise floor is the deployment of the avalanche effect in the infrared photodiode itself (APD). By applying a large bias voltage across the depletion region of the diode junction the charge generated by an absorbed photon is accelerated in the electric field of the junction and gets enough energy to generate secondary charges by impact ionization. Depending on the bandgap and the applied voltage this avalanche effect creates a charge packet of 10 to 1000 electrons per photon, which in the presence of CMOS noise is much easier to detect than a single electron. HgCdTe is an ideal material and is superior to silicon because the avalanche gain does not introduce excess noise. This means, that the noise at the input of the APD diode is equal to the noise at the output times the APD gain, whereas in silicon the excess noise factor is ~ 2 to 3. The noise-free avalanche gain in HgCdTe is due to two facts. First, the HgCdTe is a direct semiconductor and no phonons are needed for the electron to make a transition from the valence to the conduction band. Second, the mass of the electron is much smaller than the mass of the hole. Hence, for cut-off wavelengths  $\lambda_c > 2.2 \mu\text{m}$  pure electron avalanching occurs in HgCdTe and holes do not contribute to the APD gain. Therefore, they do not add noise or spread the signal response of an absorbed photon on the time axis[24].

The APD gain has already been utilized for laser-gated imaging applications by the British company SELEX for several years [25][26]. In their targeting systems they use HgCdTe eAPDs for 3-D imaging. The sensors have a cut-off wavelengths of  $\lambda_c = 4.5 \mu\text{m}$ . Making use of this experience ESO has launched a development program with SELEX to explore the applicability of this technology to IR AO wavefront sensors [27]. In laser-gated imaging applications the integration times are ~ 20ns and the dark current at large bias voltages is not relevant. However, for infrared wavefront sensing the integration times are in the millisecond range and the shot noise of the dark current of  $\lambda_c = 4.5 \mu\text{m}$  material already limits the readout noise to > 80 e-rms, even for such integration times as short as 1 ms. Hence, the goal of a pre-development study was to grow LPE HgCdTe eAPD arrays with shorter cut-off wavelengths of between  $\lambda_c$  2.4  $\mu\text{m}$  and 2.65  $\mu\text{m}$  and investigate, whether the dark current scales with wider band-gaps. The HgCdTe material was hybridized by



the loophole interconnect technology to an existing, non-optimized 320x256 pixel multiplexer developed for laser gated imaging. The pixel pitch is 24  $\mu\text{m}$  and the array has 4 video outputs operating at 5 MHz. A high speed version of NGC was developed to read out the array at 5 MHz per channel. The high speed NGC has fast clock drivers ( $T_{\text{rise}}/T_{\text{fall}} < 10\text{ns}$ ) and 8 video channels with 40 MHz pipeline ADC's [15]. Fast cryogenic CMOS preamplifiers (OPA 350) were used to amplify the video signal on the detector fan-out board. For an avalanche gain of 10 the measured dark current at 60 K is 61e/s/pixel. These results confirm that the avalanche gain and dark current of 2.65 $\mu\text{m}$  cut-off LPE/loophole diode arrays makes them suitable for AO and interferometry applications. In the ESO test camera IRATEC, which has a cold Offner relay three arrays with variable junction diameters optimized for the best signal and avalanche gain were tested. A test pattern with a grid of holes was put into the image plane and illuminated by an extended blackbody. Thus a pattern of calibrated flux was imaged onto the detector. Figure 7 shows an image taken with single DCS. The contrast in the image corresponds to 6.6 electrons/pixel. In the image on the left side of Figure 7, the APD gain of the array was set to 1 and on the right side the APD gain was 7.34. The test pattern can only be seen when the array is taking advantage of the noise-free APD gain.

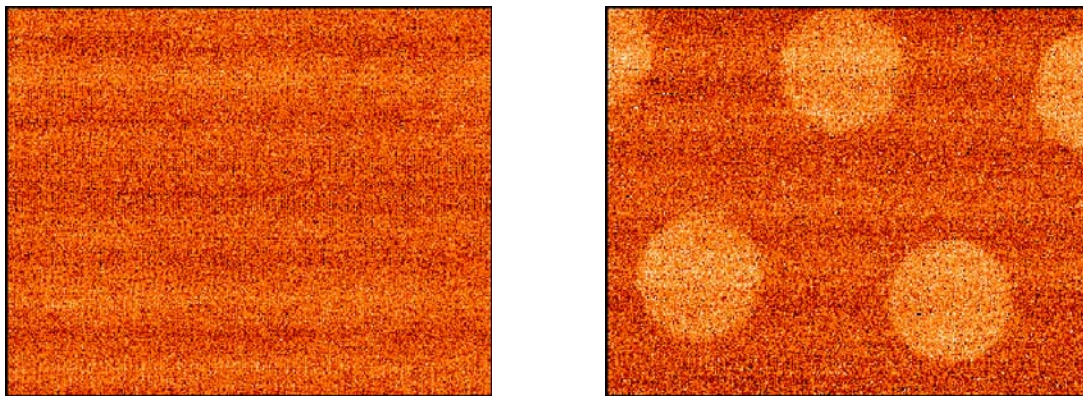


**Figure 7: Test pattern consisting of a grid of holes imaged onto APD array measured with single DCS. Average over 10 exposures. Flux contrast 6.6 electrons/pixel. Integration time 7.6 ms. Left: APD gain=1. Right: APD gain 7.34.**

Since the gain of the preamplifier in the present set-up was low (gain = 4), the readout noise was also limited by the system noise of the data acquisition system. Measurements with higher gain are planned. Notwithstanding the low gain, the multiplexer allows operation of the array in the nondestructive readout mode and reducing the readout noise by multiple sampling techniques. In Figure 8 the measured readout noise is plotted versus the number of nondestructive readouts. The expected readout noise is plotted as a dashed line. With 8 Fowler pairs the readout noise is 3 e-rms while reading out the 4 video channels with a pixel rate of 5 MHz.

The development of a multiplexer dedicated to AO wavefront sensing with 32 video outputs and windowed readout will fulfill all requirements of an infrared wavefront sensor. Extrapolating the data already obtained with the non-optimized device, as it was tested then a 32-channel multiplexer would need only 48 conversions to read 48 spectra of a fringe tracker (GRAVITY design). This would allow for 52 Fowler pairs or 104 nondestructive readouts for integration times of 1 ms, which should result in even lower readout noise than the 3 e-rms obtained with a pixel rate of 5 MHz measured with the present device.

In the framework of an extension of the current APD study we will vary the cut-off wavelength of the HgCdTe material to further explore the parameter space for the development of a specialized infrared sensor for adaptive optics and interferometry applications.

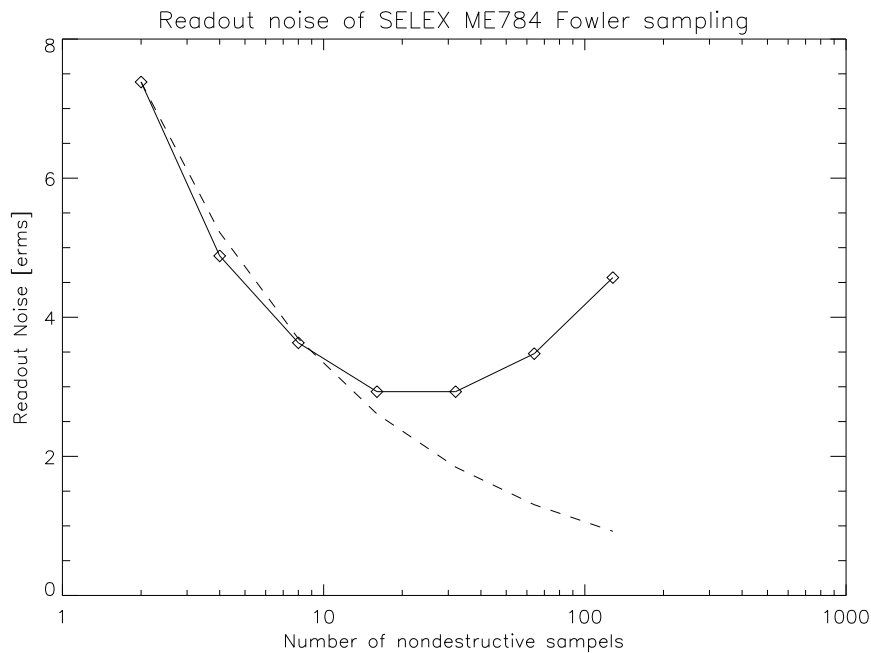


**Figure 8 Noise of SELEX eAPD array operated with ADP gain of 7.34 as a function of number of nondestructive readouts. Diamonds: measured values. Dashed: Noise DCS / SQRT(n/2) with n being the number of nondestructive readouts.**

## 10. CONCLUSIONS

Because of their excellent performance characteristics large format HgCdTe arrays have become the workhorses of second generation VLT instruments. A Mosaic with 64 Megapixels is now in routine operation at the VISTA survey telescope. Larger formats with ASIC readouts will lead the way to even larger focal planes for the ELT. A new development of 1Kx1K mid-infrared high flux devices is already producing first arrays. For high speed applications as sensors in control loops of AO systems and interferometers the most promising technique to overcome the noise barrier of CMOS multiplexers is the noise-free amplification of the signal in HgCdTe by utilizing the APD gain.

## REFERENCES

- [1] [Dietrich Baade, Andrea Balestra, Claudio Cumani, Sebastian Deiries, Mark Downing, Christoph Geimer, Evi Hummel, Olaf Iwert, Roland Reiss, Javier Reyes, and Mirko Todorovic, "Optical Detector Systems at ESO", DfA2009.](#)
- [2] [Workshop Detectors for Astronomy 2009, edited D. Baaade, ESO Garching, 12-16 October 2009.](#)
- [3] Kissler-Patig, M.; Pirard, J.-F.; Casali, M.; Moorwood, A.; Ageorges, N.; Alves de Oliveira, C.; Baksai, P.; Bedin, L. R.; Bendek, E.; Biereichel, P.; Delabre, B.; Dorn, R.; Esteves, R.; Finger, G.; Gojak, D.; Huster, G.; Jung, Y.; Kiekebush, M.; Klein, B.; Koch, F.; Lizon, J.-L.; Mehrgan, L.; Petr-Gotzens, M.; Pritchard, J.; Selman, F.; Stegmeier, J., "HAWK-I: the high-acuity wide-field K-band imager for the ESO Very Large Telescope", *Astronomy and Astrophysics*, Volume 491, Issue 3, 2008, pp.941-950, 2008.
- [4] Finger, Gert; Dorn, Reinhold J.; Eschbaumer, Siegfried; Hall, Donald N. B.; Mehrgan, Leander; Meyer, Manfred; Stegmeier, Joerg, "Performance evaluation, readout modes, and calibration techniques of HgCdTe Hawaii-2RG mosaic arrays", *Proceedings of the SPIE*, Volume 7021, pp. 70210P-70210P-13, 2008.
- [5] [Finger, G., Dorn, R., Eschbaumer, S., Ives, D., Mehrgan, L., Meyer, M., Stegmeier, J., "Recent Performance Improvements, Calibration Techniques and Mitigation Strategies for Large-format HgCdTe Arrays", DfA2009.](#)

- [6] Finger G.; Biereichel P.; Mehrgan H.; Meyer M.; Moorwood A. F.; Nicolini G.; Stegmeier J., "Infrared detector development programs for the VLT instruments at the European Southern Observatory", Proc. SPIE Vol. 3354, p. 87-98, 1998.
- [7] Dalton, G. B.; Caldwell, M.; Ward, A. K.; Whalley, M. S.; Woodhouse, G.; Edeson, R. L.; Clark, P.; Beard, S. M.; Gallie, A. M.; Todd, S. P.; Strachan, J. M. D.; Bezawada, N. N.; Sutherland, W. J.; Emerson, J. P., "The VISTA infrared camera", Proceedings of the SPIE, Volume 6269, pp. 62690X, 2006.
- [8] Bezawada N., Ives D., "Performance Overview of the VISTA IR Detectors", AASL, **336**, 499 (2005).
- [9] Mehrgan, Leander H.; Bezawada, Nagaraja; Dorn, Reinhold; Eschbaumer, Siegfried; Finger, Gert; Meyer, Manfred; Stegmeier, Joerg; Woodhouse, Guy, "256 Channel Data Acquisition System for VISTA Focal Plane to Readout Sixteen 2Kx2K Raytheon VIRGO Detectors", Scientific Detectors for Astronomy 2005, Edited by Beletic Jenna, Beletic James W. and Amico Paola, Berlin, Springer Dordrecht, p.601, 2006.
- [10] [Eso0949 – Organisation Release. "VISTA: Pioneering New Survey Telescope Starts Work"](#)
- [11] D'Odorico, Sandro; Dekker, Hans; Mazzoleni, Ruben; Vernet, Joel; Guinouard, Isabelle; Groot, Paul; Hammer, Francois; Rasmussen, Per Kjaergaard; Kaper, Lex; Navarro, Ramon; Pallavicini, Roberto; Peroux, Celine; Zerbi, Filippo Maria, "X-shooter UV- to K-band intermediate-resolution high-efficiency spectrograph for the VLT: status report at the final design review", Proceedings of the SPIE, Volume 6269, pp. 626933, 2006.
- [12] Navarro, Ramon; Elswijk, Eddy; Tromp, Niels; ter Horst, Rik; Horrobin, Matthew; Vernet, Joel; Finger, Gert; Groot, Paul; Kaper, Lex, "X-shooter near-IR spectrograph arm realization", Proceedings of the SPIE, Volume 7014, pp. 70141Y-70141Y-12, 2008.
- [13] Sharples, Ray; Bender, Ralf; Bennett, Richard; Burch, Keith; Carter, Paul; Casali, Mark; Clark, Paul; Content, Robert; Davies, Richard; Davies, Roger; Dubbeldam, Marc; Finger, Gert; Genzel, Reinhard; Haefner, Reinhold; Hess, Achim; Kissler-Patig, Markus; Laidlaw, Ken; Lehnert, Matt; Lewis, Ian; Moorwood, Alan; Muschielok, Bernard; Förster Schreiber, Natascha; Pirard, Jeff; Ramsay Howat, Suzanne; Rees, Phil; Richter, Josef; Robertson, David; Robson, Ian; Saglia, Roberto; Tecza, Matthias; Thatte, Naranjan; Todd, Stephen; Wegner, Michael, "Design of the KMOS multi-object integral-field spectrograph", Proceedings of the SPIE, Volume 6269, pp. 62691C, 2006.
- [14] Sharples, Ray, "Kmos and KMOS++", Science with the VLT in the ELT Era, Astrophysics and Space Science Proceedings, Volume . ISBN 978-1-4020-9189-6. Springer Netherlands, p. 325, 2009.
- [15] [Meyer, M., Finger, G., "Detector Data Acquisition Hardware Designs and Features of NGC \(New General Detector Controller\)", DfA2009.](#)
- [16] Beuzit, Jean-Luc; Feldt, Markus; Dohlen, Kjetil; Mouillet, David; Puget, Pascal; Wildi, Francois; Abe, Lyu; Antichi, Jacopo; Baruffolo, Andrea; Baudoz, Pierre; Boccaletti, Anthony; Carbillet, Marcel; Charton, Julien; Claudi, Riccardo; Downing, Mark; Fabron, Christophe; Feautrier, Philippe; Fedrigo, Enrico; Fusco, Thierry; Gach, Jean-Luc; Gratton, Raffaele; Henning, Thomas; Hubin, Norbert; Joos, Franco; Kasper, Markus; Langlois, Maud; Lenzen, Rainer; Moutou, Claire; Pavlov, Alexey; Petit, Cyril; Pragt, Johan; Rabou, Patrick; Rigal, Florence; Roelfsema, Ronald; Rousset, Gérard; Saisse, Michel; Schmid, Hans-Martin; Stadler, Eric; Thalmann, Christian; Turatto, Massimo; Udry, Stéphane; Vakili, Farrokh; Waters, Rens, "SPHERE: a planet finder instrument for the VLT", Proceedings of the SPIE, Volume 7014, pp. 701418-701418-12, 2008.
- [17] Hoffman, Alan; Love, Peter J.; Corrales, Elizabeth; Lum, Nancy A., "1024x1024 Si:As IBC Detector Arrays for Mid-IR Astronomy", Scientific Detectors for Astronomy 2005, Edited by Beletic Jenna, Beletic James W. and Amico Paola, Berlin, Springer Dordrecht, p.419, 2006.
- [18] Loose, Markus; Beletic, James; Garnett, James; Muradian, Norair, "Space qualification and performance results of the SIDECAR ASIC", Proceedings of the SPIE, Volume 6265, pp. 62652J, 2006.
- [19] Dorn, Reinhold J.; Eschbaumer, Siegfried; Hall, Donald N. B.; Finger, Gert; Mehrgan, Leander; Meyer, Manfred; Stegmeier, Joerg, "Evaluation of the Teledyne SIDECAR ASIC at cryogenic temperature using a visible hybrid H2RG focal plane array in 32 channel readout mode", Proceedings of the SPIE, Volume 7021, pp. 70210Q-70210Q-12, 2008.
- [20] [Dorn, R., Finger, G., Ives, D., Mehrgan, L., Meyer, M. and Stegmeier, J., "SIDECAR ASIC @ ESO", DfA2009.](#)
- [21] Finger, Gert; Smith, Roger M.; Menardi, Serge; Dorn, Reinhold J.; Meyer, Manfred; Mehrgan, Leander; Stegmeier, Joerg; Moorwood, Alan F. M., "Performance limitations of small-format high-speed infrared arrays for active control loops in interferometry and adaptive optics", Proceedings of the SPIE, Volume 5499, pp. 97-107 2004.
- [22] [Hall, Donald N.B., "Electron and Hole Avalanche Photodiode Arrays for Astronomy", DfA2009.](#)
- [23] Mehrgan, Leander H.; Eschbaumer, Siegfried; Finger, Gert; Meyer, Manfred; Stegmeier, Joerg, "Performance and evaluation of the infrared AO sensor CALICO", Proceedings of the SPIE, Volume 7021, pp. 70210W-70210W-10, 2008.

- [24] [Rothman, Johan, Mollard, L., Bisotto, S., Lefoule, X., Pistone, F. "HgCdTe avalanche photodiodes development at CEA/Leti-Minatec", DfA2009.](#)
- [25] Baker, Ian M.; Duncan, Stuart S.; Copley, Jeremy W., "A low-noise laser-gated imaging system for long-range target identification", Proceedings of the SPIE, Volume 5406, pp. 133-144, 2004.
- [26] Baker, Ian; Owton, Daniel; Trundle, Keith; Thorne, Peter; Storie, Kevin; Oakley, Philip; Copley, Jeremy, "Advanced infrared detectors for multimode active and passive imaging applications", Proceedings of the SPIE, Volume 6940, pp. 69402L-69402L-11, 2008.
- [27] [Baker, Ian, Finger, Gert. "HgCdTe Avalanche Photodiode Arrays for Wavefront Sensing and Interferometry Applications", DfA2009.](#)